Period-luminosity relations for type II Cepheids and their application

Noriyuki Matsunaga,^{1★}†‡ Michael W. Feast^{2,3} and John W. Menzies³

Accepted 2009 April 29. Received 2009 April 29; in original form 2009 March 24

ABSTRACT

JHK_s magnitudes corrected to mean intensity are estimated for Large Magellanic Cloud (LMC) type II Cepheids in the OGLE-III survey the third phase of the Optical Gravitational Lensing Experiment (OGLE). Period-luminosity (PL) relations are derived in JHKs as well as in a reddening-free VI parameter. Within the uncertainties, the BL Her stars (P < 4 d) and the W Vir stars (P = 4 to 20 d) are colinear in these PL relations. The slopes of the infrared relations agree with those found previously for type II Cepheids in globular clusters within the uncertainties. Using the pulsation parallaxes of V553 Cen and SW Tau, the data lead to an LMC modulus uncorrected for any metallicity effects of 18.46 ± 0.10 mag. The type II Cepheids in the second-parameter globular cluster, NGC 6441, show a PL(VI) relation of the same slope as that in the LMC, and this leads to a cluster distance modulus of 15.46 ± 0.11 mag, confirming the hypothesis that the RR Lyrae variables in this cluster are overluminous for their metallicity. It is suggested that the Galactic variable κ Pavonis is a member of the peculiar W Vir class found by the OGLE-III group in the LMC. Low-resolution spectra of OGLE-III type II Cepheids with P > 20 d (RV Tau stars) show that a high proportion have TiO bands; only one has been found showing C2. The LMC RV Tau stars, as a group, are not colinear with the shorter period type II Cepheids in the infrared PL relations in marked contrast to such stars in globular clusters. Other differences between LMC, globular cluster and Galactic field type II Cepheids are noted in period distribution and infrared colours.

Key words: stars: distances – stars: Population II – Cepheids – stars: variables: other – Magellanic Clouds – infrared: stars.

1 INTRODUCTION

Type II Cepheids (CephIIs) have periods in the same range as classical Cepheids but are lower mass stars belonging to disc and halo populations. They are conventionally divided into three period groups: BL Her (BL) stars at short periods, W Vir (WV) stars at intermediate periods and RV Tau (RV) stars at the longest periods. The period divisions tend to be somewhat arbitrary. In a recent paper to which considerable reference will be made, Soszyński et al. (2008, hereafter S08) adopt divisions at 4 and 20 days, and we follow these thresholds here. The RV stars tend to show alternating deep and shallow minima (and this is often taken as a defining characteristic), but the single period of the RV stars will be used in this paper as in S08. In addition to the BL, WV and RV stars, S08 define an ad-

Osawa, Mitaka, Tokyo 181-0015, Japan.

 $\ddagger Research$ fellow of the Japan Society for the Promotion of Science.

ditional class of peculiar W Vir (pW) stars which will be discussed below.

Most workers have accepted the evolutionary scheme elaborated by Gingold (Gingold 1976, 1985). In this, the BL stars are evolving from the (blue) horizontal branch towards the lower asymptotic giant branch (AGB). The WV stars are on loops to the blue from the AGB and the RV stars are moving to the blue in a post-AGB phase. Matsunaga et al. (2006, hereafter M06) showed that the CephIIs in globular clusters defined narrow period–luminosity (PL) relations in the near-infrared bands, JHK_s , with little evidence for a metallicity effect in these relations. This suggests that these stars may be useful distance indicators for disc and halo populations. Pulsation parallaxes of Galactic CephIIs were used by Feast et al. (2008, hereafter F08) to calibrate these cluster PL relations and to discuss the distances of the Large Magellanic Cloud (LMC) and the Galactic Centre.

This paper discusses the CephIIs in the LMC based on the recent optical OGLE-III survey (S08) and the results of the near-infrared survey with the Infrared Survey Facility (IRSF). The CephIIs in the second-parameter cluster NGC 6441 and those around the Galactic

¹Department of Astronomy, Kyoto University, Kitashirakawa-Oiwake-cho, Sakyo-ku, Kyoto 606-8502, Japan

²Department of Astronomy, University of Cape Town, 7701, Rondebosch, South Africa

³South African Astronomical Observatory, PO Box 9, 7935, Observatory, South Africa

^{*}E-mail: matsunaga@ioa.s.u-tokyo.ac.jp †Present address: Institute of Astronomy, University of Tokyo, 2-21-1

Centre are also discussed as well as the nature of the CephII variable κ Pav.

2 INFRARED PHOTOMETRY

S08 catalogued 197 CephII variables in the LMC. We searched for near-infrared counterparts in the IRSF catalogue (Kato et al. 2007). This is a point-source catalogue in JHK_s of 40 deg 2 of the LMC, 11 deg 2 of the Small Magellanic Cloud and 4 deg 2 of the Magellanic Bridge. The catalogue is based on simultaneous images in JHK_s obtained with the 1.4-m IRSF telescope and the Simultaneous 3-colour Infrared Imager for Unbiased Survey (SIRIUS) based at the South African Astronomical Observatory (SAAO), Sutherland. The 10σ limiting magnitudes of the survey are 18.8, 17.8 and 16.6 mag for J, H and K_s . The catalogue extends to fainter magnitudes and has higher resolution than the point-source catalogue of the Two-Micron All-Sky Survey (2MASS; Skrutskie et al. 2006) in the region of the Magellanic Clouds.

We found matches for 188 S08 CephII sources with a tolerance of 0.5 arcsec. The differences in coordinate are small between the catalogues with a standard deviation of less than 0.1 arcsec in both Right Ascension and Declination. Among nine sources without IRSF counterparts, seven (1–3, 194–197) are located outside of the IRSF survey field. There are no counterparts around the two BL stars (69 and 123) probably because they are too faint. These variables actually have the shortest periods among our sample. On the other hand, we found two IRSF counterparts for 15 S08 sources: these

IRSF counterparts were detected in neighbouring fields of the IRSF survey as listed in Table 1.

IRSF magnitudes in all three bands are not available for nine BL stars and one pW star. In most of the cases, K_s -band magnitudes are missing because of the faintness of the short-period BL stars. H-band magnitudes are unavailable for No. 40 (pW) and 144 (BL); the reason for this is unclear.

Since S08 give the periods and dates of maximum light in I (= phase zero), we can derive the phases (between zero and one) of the single JHK_s observations. Using the I-band light curves, we obtain the value of I at that phase and its difference from the intensity mean value, $\langle I \rangle$. Assuming that the light curves in JHK_s are similar to those in I, we obtain an estimate of the mean (phase-corrected) magnitude in each infrared band.

In order to check the validity of the above assumption, we use the S08 sources with two IRSF counterparts. There are 15 such sources (two RV, seven WV, six BL stars). We list the dates, phases and observed magnitudes from the two IRSF measurements in Table 1. For each phase at which the IRSF survey was conducted, we also estimate a predicted *I*-band magnitude by taking a mean of the *I*-band measurements which were made within ± 0.05 of the phase of the IRSF survey. Variations between two IRSF measurements $(\Delta J, \Delta H, \Delta K_s)$ have the same signs as the difference between the predicted *I*-band magnitudes (ΔI) for each object. Fig. 1 plots the variations of the IRSF measurements against ΔI . This clearly shows that the variations in JHK_s reasonably agree with those in I, except for the ΔK_s values for BL stars (crosses) which have large error

Table 1. The LMC CephIIs with two IRSF measurements. MJD, pulsation phase of the observations and JHK_s magnitudes and their errors are listed for each IRSF entry. Also indicated are I-band magnitudes at the phases of the IRSF measurements based on the OGLE light curves.

OGLE-	Type	$\log P$	IRSF counterpart								Expected I	
ID			IRSF-Field	MJD(obs)	Phase	J	E_J	Н	E_H	$K_{\rm s}$	E_K	
10	BL Her	0.17695	LMC0456-6840I	53062.869	0.681	17.71	0.04	17.35	0.04	17.23	0.25	18.26
10			LMC0452-6840G	53049.895	0.049	17.33	0.03	17.06	0.04	16.90	0.17	17.70
11	RV Tau	1.593 91	LMC0453-6740G	52683.765	0.578	13.71	0.03	13.32	0.03	13.25	0.02	14.17
11			LMC0454-6720A	53017.960	0.091	13.42	0.01	13.12	0.01	13.03	0.02	14.03
22	W Vir	1.03006	LMC0458-7040G	53497.695	0.076	15.44	0.02	15.05	0.02	15.04	0.03	16.13
22			LMC0502-7040I	53117.759	0.623	15.75	0.02	15.34	0.02	15.29	0.03	16.38
38	W Vir	0.603 54	LMC0503-6840A	53123.751	0.964	15.94	0.02	15.87	0.02	15.84	0.05	16.10
38			LMC0507-6840C	53341.916	0.320	15.85	0.01	15.66	0.02	15.66	0.05	16.09
50	RV Tau	1.540 93	LMC0511-6840C	53051.855	0.304	14.35	0.02	14.03	0.02	13.82	0.02	14.93
50			LMC0511-6900I	52612.916	0.672	14.65	0.03	14.30	0.02	14.10	0.02	15.07
59	W Vir	1.223 65	LMC0510-7040G	53322.877	0.012	14.68	0.01	14.36	0.01	14.22	0.02	15.28
59			LMC0514-7040I	52714.762	0.677	15.42	0.02	15.05	0.02	15.01	0.04	15.90
76	BL Her	0.323 11	LMC0518-6820I	52657.914	0.487	17.19	0.03	16.77	0.03	16.64	0.09	17.85
76			LMC0514-6820G	52660.786	0.852	17.51	0.05	17.14	0.07	17.05	0.16	18.09
100	W Vir	0.871 05	LMC0522-7020F	53355.891	0.554	16.31	0.02	16.01	0.02	16.01	0.08	16.83
100			LMC0522-7020E	52700.891	0.411	16.13	0.02	15.79	0.02	15.91	0.06	16.71
105	BL Her	0.17298	LMC0522-7020E	52700.891	0.040	17.05	0.03	16.84	0.03	16.74	0.14	17.32
105			LMC0522-7020H	52701.758	0.622	17.63	0.07	17.13	0.07	16.92	0.21	17.93
118	W Vir	1.103 76	LMC0525-6800B	52673.837	0.240	15.44	0.02	15.00	0.02	14.90	0.03	16.30
118			LMC0525-6820H	52683.781	0.023	15.12	0.03	14.74	0.02	14.58	0.03	15.81
122	BL Her	0.187 15	LMC0525-6840H	52683.954	0.007	17.46	0.04	17.14	0.04	17.10	0.22	18.05
122			LMC0525-6820B	52675.910	0.779	17.73	0.04	17.48	0.08	17.14	0.18	18.33
138	BL Her	0.144 14	LMC0529-6840A	52684.777	0.524	17.29	0.10	17.43	0.10	16.52	0.13	18.23
138			LMC0529-6900G	52364.819	0.931	17.11	0.08	17.20	0.07	16.99	0.14	17.92
143	W Vir	1.163 47	LMC0529-6920G	52363.769	0.569	15.57	0.02	15.27	0.02	15.17	0.04	16.21
143			LMC0533-6920I	53331.899	0.014	14.86	0.03	14.52	0.02	14.44	0.02	15.47
146	W Vir	1.003 44	LMC0533-6840C	52687.758	0.228	15.63	0.02	15.25	0.02	15.12	0.03	16.39
146			LMC0533-6900I	52286.935	0.463	15.88	0.01	15.51	0.02	15.35	0.03	16.50
148	BL Her	0.42679	LMC0533-6920C	52969.042	0.572	17.13	0.02	16.85	0.02	16.66	0.07	17.73
148			LMC0533-6940I	52226.973	0.824	16.84	0.02	16.67	0.04	16.57	0.10	17.33

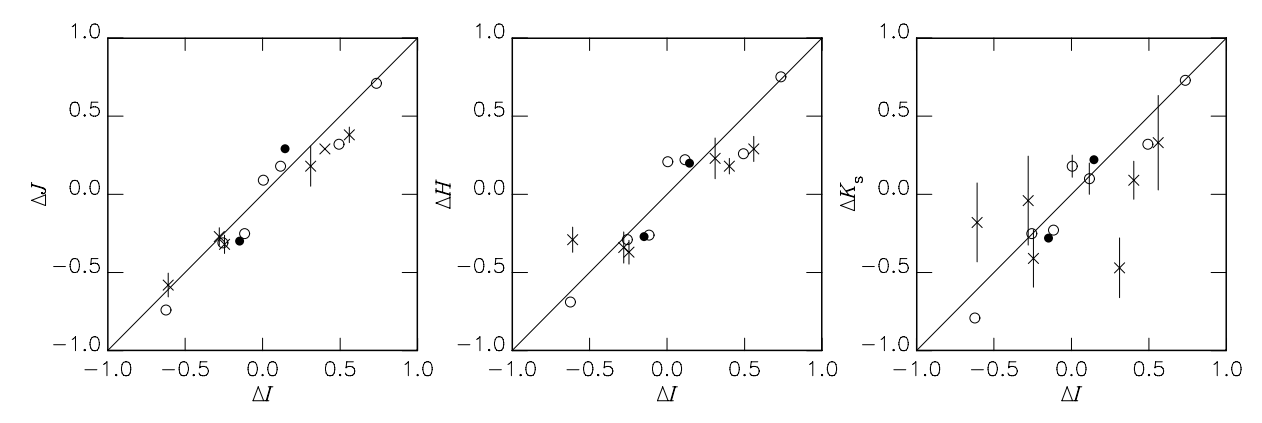


Figure 1. Differences of JHK_s magnitudes at two epochs of the IRSF observations are plotted against those of I-band magnitudes estimated from the OGLE light curves. Crosses indicate BL, open circles WV and filled circles RV stars. The error bars are omitted when their sizes are smaller than the symbols.

Table 2. The first 10 lines of the catalogue of S08 sources with IRSF counterparts. This is a sample of the full version, which is available in the online version of the article (see Supporting Information). MJD, pulsation phase of the observations, JHK_s magnitudes and their errors are listed for each IRSF measurement as well as the OGLE-IDs, types and periods. Shifts for the phase corrections obtained from the I-band light curves are also listed if available. Nine S08 sources are absent because their IRSF counterparts were not found, and 15 S08 sources are listed twice because they are identified with two counterparts from neighbouring fields of the IRSF survey.

OGLE-	Туре	$\log P$	IRSF counterpart									δ_{ϕ}
ID		_	IRSF-Field	MJD(obs)	Phase	\overline{J}	E_J	Н	E_H	$K_{\rm s}$	E_K	,
4	BL Her	0.28240	LMC0446-6800C	52645.086	0.121	16.64	0.04	16.33	0.06	16.27	0.11	0.203
5	RV Tau	1.52095	LMC0447-7000G	53037.995	0.161	13.82	0.02	13.41	0.02	13.28	0.03	0.201
6	BL Her	0.03660	LMC0450-6720B	53031.900	0.273	17.63	0.04	17.43	0.07	17.32	0.22	0.047
7	BL Her	0.09435	LMC0452-6920F	53044.963	0.224	17.50	0.04	17.25	0.06	_	_	-0.005
8	BL Her	0.24207	LMC0451-7000E	53308.910	0.293	17.25	0.02	17.34	0.06	17.31	0.17	0.130
9	BL Her	0.245 84	LMC0454-6700C	53365.791	0.222	17.21	0.04	16.82	0.06	16.92	0.19	0.069
10	BL Her	0.17695	LMC0456-6840I	53062.869	0.681	17.71	0.04	17.35	0.07	17.23	0.25	-0.281
10	BL Her	0.17695	LMC0452-6840G	53049.895	0.049	17.33	0.03	17.06	0.04	16.90	0.17	0.278
11	RV Tau	1.593 91	LMC0453-6740G	52683.765	0.578	13.71	0.03	13.32	0.02	13.25	0.02	_
11	RV Tau	1.593 91	LMC0454-6720A	53017.960	0.091	13.42	0.01	13.12	0.01	13.03	0.02	-

bars. That is, these observations are consistent with the assumption that the JHK_s light curves are, to a first approximation, similar to those at I and have about the same amplitude.

Light curves of RV stars often have a large scatter, and it is difficult to make satisfactory phase corrections. We selected eight RV stars which have good light curves, i.e. 5, 58, 104, 115, 125, 135, 169 and 192, and use these light curves to make phase corrections. For pW stars, we do not try to correct the phase effect, and they are not included in the following discussions of the PL relation.

We here present a catalogue of the S08 sources with the IRSF counterparts in Table 2, where the JHK_s values are those listed in the IRSF catalogue (Kato et al. 2007). The indicated errors, E_J , E_H and E_K , are taken from their catalogue. The quantity δ_ϕ is the correction which must be added to the I magnitude at the epoch of the IRSF observation to correct it to the intensity mean magnitude and is the value we adopt to correct the infrared magnitudes to means. Note that we list those with IRSF counterparts in neighbouring fields twice.

3 PERIOD-LUMINOSITY RELATIONS

3.1 General and optical relations

In this section, we discuss the optical PL relations using the data in S08. Based on notes given by S08, the following stars were omitted in all solutions, optical and infrared: 88, 153, 166, 185

(blends), 21, 23, 52, 77, 84, 93, 98 (eclipsing), 50 (too blue), 108 (low amplitude), 113 (scatter in light curve), 51 (variable amplitude) and 150 (variable mean magnitude).

The general features of CephII optical PL diagrams are well shown in fig. 1 of S08. The plots of V and I against $\log P$ show considerable scatter and clear non-linearity. Introduction of a colour term [W = I - R(V - I)] with R = 1.55 produces a rather narrow and nearly linear PL(W) relation for the BL and WV stars although there is still scatter amongst the RV stars.

S08 recognize a class of pW stars. These have distinctive light curves, and a high proportion are binaries. Many of these lie above (brighter than) the normal WV stars in the various PL plots. In the solutions below, all the pW stars are omitted. There are also a few stars in the BL period range which lie brighter than the majority of the BL stars in the PL(W) plot and in the region occupied by anomalous Cepheids. We have chosen to omit these stars (107, 114, 142, 153, 166) in our work.

If the value of R is correctly chosen, W is a reddening-free parameter. Udalski et al. (1999) found R = 1.55 as appropriate to the OGLE-II photometry from the results of Schlegel, Finkbeiner & Davis (1998). On the other hand, a value of R = 1.45 has frequently been used (e.g. Freedman et al. 2001; van Leeuwen et al. 2007). This latter value is based on the extinction law of Cardelli, Clayton & Mathis (1989). We give below results based on both values of R. In the work with very heavily reddened stars, the exact value of R may become important.

For 55 BL stars, we find

$$W_1 = I - 1.55(V - I) = -2.598(\pm 0.094)(\log P - 0.3) + 16.597(\pm 0.017), (\sigma = 0.104),$$
(1)

and

$$W_2 = I - 1.45(V - I) = -2.572(\pm 0.093)(\log P - 0.3) + 16.665(\pm 0.016), (\sigma = 0.103).$$
(2)

For 76 WV stars, we find

$$W_3 = I - 1.55(V - I) = -2.564(\pm 0.073)(\log P - 1.2) + 14.333(\pm 0.019), (\sigma = 0.108),$$
(3)

and

$$W_4 = I - 1.45(V - I) = -2.551(\pm 0.073)(\log P - 1.2) + 14.431(\pm 0.019), (\sigma = 0.105).$$
(4)

The slopes and (effective) zero-points do not differ significantly between the solutions for BL and WV stars, so that we give solutions for BL+WV stars:

$$W_5 = I - 1.55(V - I) = -2.521(\pm 0.022)(\log P - 1.2) + 14.339(\pm 0.015), (\sigma = 0.105),$$
(5)

and

$$W_6 = I - 1.45(V - I) = -2.486(\pm 0.022)(\log P - 1.2) + 14.440(\pm 0.15), (\sigma = 0.106).$$
(6)

These relations are narrow ($\sigma \sim 0.1$) as expected from Fig. 1 of S08.

Use of the PL(W) relation brings stars that lie below the bulk of the CephIIs in the $\log P - V$ (and I) diagrams and are redder than the bulk of the CephIIs PL into agreement with the others as expected for reddening-free relations. In addition, we can expect that, as with classical Cepheids, CephIIs occupy an instability strip of finite width in temperature (i.e. colour). Thus, a PL relation has a finite scatter and a colour term is needed to reduce this. In the case of the classical Cepheids, the coefficient of the required colour term is about 1.45 (Udalski et al. 1999; van Leeuwen et al. 2007) so that W corrects in that case for both reddening and strip width.

As a first approximation, we might expect the same value of R to apply in the case of the CephIIs. One can test this by looking at the residual from the PL(W) relation of the bluest stars, since it seems unreasonable to assume that the bulk of the BL stars which scatter around (V-I) ~ 0.7 are heavily reddened by interstellar extinction. There are eight BL stars bluer than (V-I) = 0.5 which were not discarded for any of the reasons given above (stars 6, 20, 41, 71, 89, 102, 136 and 145). Their residuals from the above equation for W_2 are 0.000, +0.084, -0.029, -0.145, +0.100, -0.081, +0.305 and -0.066, respectively, giving a mean of +0.021 \pm 0.050 or -0.020 \pm 0.033 if No. 136 is omitted. The residual for 136 is rather large, and this is the bluest star in the sample. It seems possible that this might be a blend or a binary like some of the rejected stars, but this is not certain.

Taking the above results together with the colour–magnitude diagram of S08 (their fig. 2) strongly suggests that the BL stars occupy an instability strip with a width of \sim 0.4 mag in V-I. The exact limits to the strip are not clearly defined. However, it is important for the zero-point calibration discussed in Section 4 that for an intrinsic width of this order the PL(W) relation remains narrow, indicating that in this case (as for classical Cepheid) the relation corrects well for both reddening and intrinsic colour variation.

Fig. 2 of S08 also suggests that, if the pW stars are omitted, most of the WV stars occupy a narrower instability strip than the BL

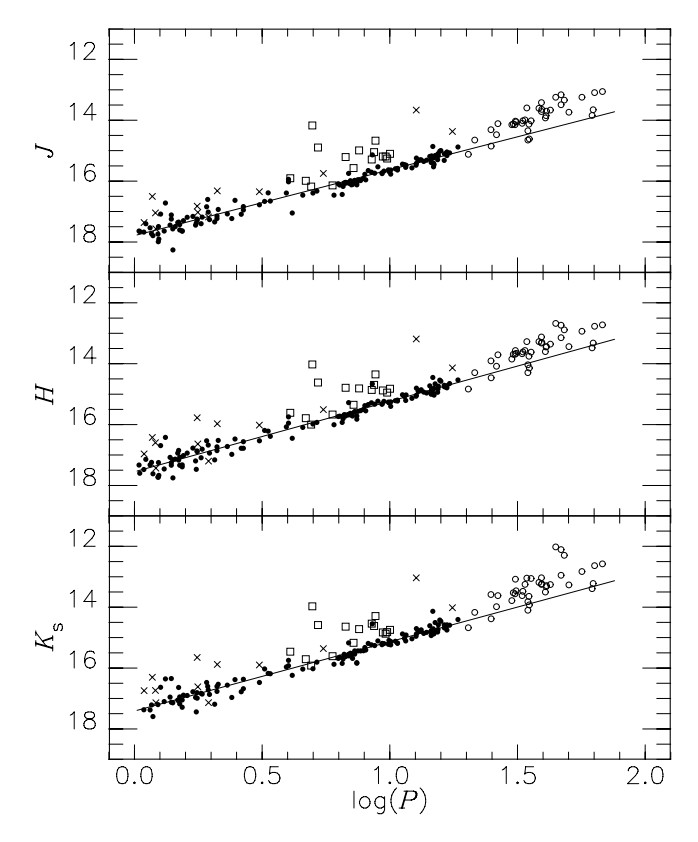


Figure 2. Period–magnitude relation of CephIIs in the LMC. The phase-corrected JHK_s magnitudes are plotted against periods. Filled circles indicate BL+WV stars used to solve the PL relations, while crosses indicate those excluded, open squares pW and open circles RV stars.

stars, though it is uncertain whether or not the colours of some of the redder WV stars are due to interstellar reddening or are intrinsic.

3.2 Infrared PL relations

Fig. 2 plots the phase-corrected JHK_s magnitudes against $\log P$ for the LMC CephIIs. Note that only a few of the RV stars have phase corrections applied. In this section, we give infrared PL relations for the BL and WV stars using the phase-corrected data. It is evident from Fig. 2 that the RV stars do not continue the linear PL relations to longer periods. They are discussed in Section 5.2.

Least-square solutions yield the following relations. For BL stars,

$$J_1 = -2.164(\pm 0.240)(\log P - 0.3) + 17.131(\pm 0.038),$$

$$(\sigma = 0.25, 55 \text{ stars})$$
(7)

$$H_1 = -2.259(\pm 0.248)(\log P - 0.3) + 16.857(\pm 0.039),$$

 $(\sigma = 0.26, 54 \text{ stars})$ (8)

$$K_{s,1} = -1.992(\pm 0.278)(\log P - 0.3) + 16.733(\pm 0.040),$$

 $(\sigma = 0.26, 47 \text{ stars}).$ (9)

For WV stars, we find

$$J_2 = -2.337(\pm 0.114)(\log P - 1.2) + 15.165(\pm 0.030),$$

(\sigma = 0.18, 82 stars) (10)

$$H_2 = -2.406(\pm 0.100)(\log P - 1.2) + 14.756(\pm 0.027),$$

 $(\sigma = 0.16, 82 \text{ stars})$ (11)

$$K_{s,2} = -2.503(\pm 0.109)(\log P - 1.2) + 14.638(\pm 0.029),$$

 $(\sigma = 0.17, 82 \text{ stars}).$ (12)

The greater scatter for the BL stars compared with the WV stars is at least partly due to the poorer photometry for the fainter (BL) stars, especially at the longer wavelengths. Given the uncertainties in the slopes, there is no evidence for difference between the BL and WV stars and the following are joint solutions:

$$J_3 = -2.163(\pm 0.044)(\log P - 1.2) + 15.194(\pm 0.029),$$

(\sigma = 0.21, 137 stars) (13)

$$H_3 = -2.316(\pm 0.043)(\log P - 1.2) + 14.772(\pm 0.028),$$

 $(\sigma = 0.20, 136 \text{ stars})$ (14)

$$K_{s,3} = -2.278(\pm 0.047)(\log P - 1.2) + 14.679(\pm 0.029),$$

 $(\sigma = 0.21, 129 \text{ stars}).$ (15)

The slopes do not differ significantly from those found by M06 for CephIIs in globular clusters except possibly at K_s where, for instance, the slope in equation (15) is shallower by 1.9σ compared with the cluster value. The LMC result is sensitive to whether we reject or retain some of the fainter BL stars. In the shortest period range, the detection limit of the IRSF survey can introduce a bias in the PL diagram. In fact, all the stars with the IRSF K_s missing are BL stars with P shorter than 1.5 days. The slope gets steeper and agrees with the case of WV (equation 12) if we use only those with P > 1.5 d. Since the difference is in any case only of marginal significance, we have chosen to ignore it. Then, adopting the cluster slopes we obtain the following relations for the combined BL and WV star set:

$$J_4 = -2.230(\pm 0.05)(\log P - 1.2) + 15.160(\pm 0.018),$$

(\sigma = 0.21) (16)

$$H_4 = -2.340(\pm 0.05)(\log P - 1.2) + 14.760(\pm 0.017),$$

($\sigma = 0.20$) (17)

$$K_{s,4} = -2.410(\pm 0.05)(\log P - 1.2) + 14.617(\pm 0.015),$$

 $(\sigma = 0.21),$ (18)

where the uncertainties in the slopes are those given by M06.

Solutions have also been made using the LMC JHK_s data uncorrected for phase. In the case of the WV stars, the scatters (σ) about equations analogous to (10), (11) and (12) are 0.26, 0.23 and 0.24 mag, respectively. This may be compared with the figures for the phase-corrected data: 0.18, 0.16 and 0.17 mag. Thus, a significant improvement is found using the phase-corrected data and the scatter becomes comparable with that found by M06 for CephII in globular clusters (0.16, 0.15 and 0.14) even though the LMC results depend on a single observation per star and no allowance is made for possible differential reddening. A similar test in the case of the BL stars shows little decrease in the scatter when the phase-corrected rather than uncorrected data are used. This is probably due to the poorer quality of the photometry for these fainter stars as already noted

4 PL CALIBRATION AND APPLICATIONS

4.1 The LMC

The various PL relations discussed above can be calibrated using the two Galactic BL stars with pulsation parallaxes V553 Cen (log P =

Table 3. Estimates of the distance modulus of the LMC (μ_{LMC}) based on pulsation parallaxes of V553 Cen and SW Tau combined with the PL relations in this paper.

Eq.	$\mu_{ ext{LMC}}$	Note
(1)	18.45	$W_1(R = 1.55)$
(2)	18.45	$W_2(R=1.45)$
(7)	18.47	J_1
(8)	18.42	H_1
(9)	18.41	$K_{s,1}$
(7)–(9)	18.44	Mean $(J_1, H_1, K_{s,1})$
(16)	18.51	J_4
(17)	18.44	H_4
(18)	18.48	$K_{s,4}$
(16)–(18)	18.48	Mean $(J_4, H_4, K_{s,4})$

0.314) and SW Tau (log P = 0.200) (see F08). The intrinsic colours of these stars are $(V - I)_0 = 0.70$ and 0.36. This corresponds to 0.80 and 0.46 if we redden them by an amount expected in the LMC, where we adopt as a typical mean reddening, $E_{B-V} = 0.074$ (see Caldwell & Coulson 1985). Thus, these two stars span almost the whole range suggested above for the width of the BL instability strip.

Using the data of tables 4 and 5 of F08, we can calibrate the zero-points of the various PL relations and hence estimate the modulus of the LMC (μ_{LMC}). In doing this, the *JHK* data of F08 were converted from the SAAO system into that of the IRSF using the transformations from SAAO to 2MASS (Carpenter 2001 and web site updates) and those from 2MASS to IRSF using the relations of Kato et al. (2007). We obtain μ_{LMC} estimates between 18.41 and 18.51 based on different PL relations obtained above as listed in Table 3.

The uncertainties to be associated with these values are of interest. The uncertainties estimated for the distance moduli of V553 Cen and SW Tau are each 0.08 (F08). This thus contributes 0.06 to the uncertainties in the above mean results. In fact the W zero-points derived from the two stars differ by 0.2 mag, i.e. an uncertainty in the mean of 0.10. On the other hand, the two stars give mean zero-points for the JHK_s relations with formal uncertainties of only \sim 0.04 mag. These figures of course have their own, considerable, uncertainty. However, remembering the range in intrinsic (V-I) of the two stars, they suggest very narrow JHK_s PL relations. The scatter quoted above for the infrared PL relations must be largely due to observational effects, especially in the case of the BL stars.

Taken together these results suggest μ_{LMC} of 18.46 mag. They also suggest an uncertainty of less than 0.10 mag, but to be reasonably conservative we adopt this as the standard error. No account of any possible metallicity effects is taken in this. These values agree well with those derived from classical Cepheids with trigonometrical parallaxes by van Leeuwen et al. (2007) and Benedict et al. (2007). These authors found 18.52 \pm 0.03 from a PL(W) relation and 18.47 \pm 0.03 from a PL(K_s) relation again without metallicity corrections. In the case of the PL(W) relation, this gave a modulus of 18.39 ± 0.05 when a recent metallicity correction (Macri et al. 2006) was applied, though this correction has been questioned (Bono et al. 2008). These results suggest that any metallicity correction to the PL(W) result for CephIIs will be small. M06 found no evidence for a metallicity correction to the JHK_s PL relations based on globular clusters. Current theoretical work (Bono, Caputo & Santolamazza 1997; Di Criscienzo et al. 2007) suggests that the evolutionary and pulsational properties of CephIIs are only minimally affected by metallicity.

4.2 The distance to the Galactic Centre

The distance to the Galactic Centre (R_0) based on the CephIIs in the Galactic bulge was discussed in F08 on the basis of the parallaxes of V553 Cen and SW Tau and the K-band observations of Groenewegen, Udalski & Bono (2008). A value of $R_0 = 7.64 \pm 0.21$ kpc was obtained. The quoted standard error does not take into account any systematic error in the corrections for reddening adopted by Groenewegen et al. (2008). These corrections are substantial and this may lead to a significant uncertainty in the method. It is possible, in principle, to use reddening-free relations. Groenewegen et al. illustrated this using the colour (I - K). However, in view of the high reddening of the stars used, the result is very sensitive to the coefficient used in the reddening-free relation (equivalent to R in Section 3.1). Infrared colours (e.g. J - K or H - K) may be more successful when the relevant data are available.

4.3 NGC 6441

NGC 6441 is an outstanding example of a 'second-parameter' globular cluster. It is of relatively high metallicity ([Fe/H] = -0.53) but has an extended horizontal branch and RR Lyrae variables. The RR Lyraes seem to be evolved and brighter than expected for their metallicity (Pritzl et al. 2003, hereafter P03). The cluster also contains CephIIs for which P03 give VI photometry. The reddening is large, $E_{B-V} = 0.51$ according to P03, and possibly uncertain. This is therefore a useful cluster to study with a reddening-free parameter. A solution of the data for the seven CephIIs, taking W = I - 1.45(V - I), is

$$W = -2.549(\pm 0.040) \log P + 14.439(\pm 0.044). \tag{19}$$

The slope is not significantly different from that found for the LMC CephIIs. Calibrating this relation using the data on V553 Cen and SW Tau leads to a cluster modulus of 15.46 \pm 0.11 mag. This is very close to the value (15.48) adopted by P03 on the assumptions that the RR Lyraes in this metal-rich cluster have absolute magnitudes similar to those with [Fe/H] \sim -2.0 and that $E_{B-V}=0.51$. Note however that the visual absolute magnitudes of the RR Lyraes depend critically on the reddening adopted.

M06 list mean JHK_s values for two CephIIs in NGC 6441. However, one of these (V129) may be affected by blending (see Section 5.1), and we omit this star. The data on the other star (V6) can be used together with the PL relations in M06 and the data on V553 Cen and SW Tau to obtain another estimate of the modulus. Adopting the same reddening as above, we obtain a modulus of 15.49 ± 0.05 consistent with the value just given from PL(W). This infrared modulus also depends on the adopted reddening. However, this cannot be made much smaller if the intrinsic colours of the NGC 6441 CephIIs, $(V-I)_0$, are similar to those of the LMC CephIIs.

4.4 κ Pavonis

 κ Pavonis (κ Pav; log P=0.959) has long been thought of as probably the nearest CephII, and hence a prime candidate for fixing the distance scale for these objects. However, the results given in F08 were puzzling. An apparently good pulsation parallax with a small error was derived leading to a distance modulus of 6.55 ± 0.07 .

The revised *Hipparcos* parallax led to a modulus of 5.93 ± 0.26 : a 2σ difference from the pulsation parallax. It was recognized in F08 that the pulsation parallax implied that the star was brighter than expected for a CephII. If we adopt a LMC modulus of 18.5, the star is 0.40 mag brighter than the LMC PL(W) relation at its period, 0.52 mag brighter than the PL(J) relation and 0.43 mag brighter than the PL(K_s) relation. If the LMC is closer than 18.5 mag, as suggested above, these differences will be increased.

Comparison of the data for κ Pav (table 5 of F08) with fig. 1 of S08 shows that in V and I as well as W the star lies above the normal CephII stars and in the region of the pW stars which was identified by S08. Further evidence that κ Pav belongs to the pW class is given by its colour. Its intrinsic colour is $(V-I)_0=0.66$, hence (V-I)=0.76 if the star is reddened by an amount comparable with the LMC stars. Comparison with the data of S08 (e.g. their fig. 2) shows that these colours are bluer than normal CephIIs of this period (WV stars) and fall in the region occupied by the pW stars.

There are two further indications that κ Pav belongs to the pW class. The revised *Hipparcos* data discussed in F08 indicate that the star probably had a close companion. This is consistent with the fact that S08 find a high proportion, and probably all, of pW variables are binaries. Finally, S08 pick out pW stars based on their light curves, the rising branch being steeper than the declining one. Comparison of the light curve of κ Pav = HIP 093015 (ESA 1997, Vol. 12) with the examples in S08 (fig. 5) strongly suggests that it should be classed with the pW variables.

5 THE INFRARED COLOURS OF TYPE II CEPHEIDS

In this section, we discuss and compare the infrared colours of CephIIs in the LMC and those in globular clusters (Section 5.1 for BL and WV stars, and 5.2 for RV stars). This section is essentially descriptive and further data are required (for instance on the metallicities of the LMC stars) before detailed interpretation of the phenomena noted can be made.

Fig. 3 presents the colour-magnitude diagram in panel (a) and colour-colour diagrams in panels (b), (c) and (d) for BL, WV+pW and RV variables, respectively. Symbols are as in Fig. 2, and the uncertainties in colour are indicated by error bars if they exceed the size of the symbols. We also plot CephIIs in globular clusters (M06) in the colour-colour diagram using grey star symbols, and Galactic RV stars from Lloyd Evans (1985) in panel (d) with triangles. The magnitudes of the latter sample were converted from the SAAO system to that of the IRSF as described in Section 4.1. No reddening corrections were applied to the LMC objects and the Galactic ones, while, for the cluster variables, the dereddened colours have been adjusted for the mean LMC reddening ($E_{B-V} = 0.074$ mag assumed as in Section 4.1). The curve in the two-colour plots is the location of normal giants (G0III-K5III) from Bessell & Brett (1988) whose colours are also transformed into the IRSF/SIRIUS system after adding LMC reddening.

The infrared colour/log *P* relations are plotted in Fig. 4. Symbols are the same as in Fig. 3, but the Galactic RV stars are not included. As in the colour–colour plots, the dereddened magnitudes of the globular-cluster objects have been reddened by an amount corresponding to the adopted LMC reddening, so that the two samples are directly comparable. Discussions on these diagrams are given below.

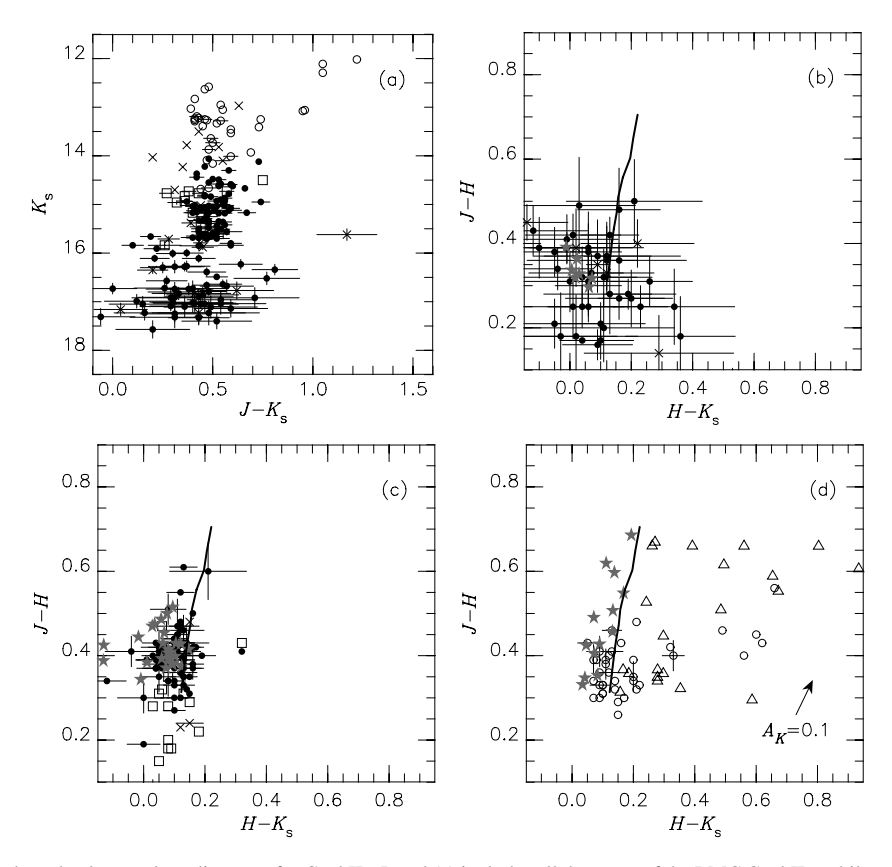


Figure 3. Colour–magnitude and colour–colour diagrams for CephIIs. Panel (a) includes all the types of the LMC CephIIs, while panels (b), (c) and (d) are for BL, WV+pW and RV stars, respectively. Symbols are the same as in Fig. 2 for the LMC objects, while those in globular clusters are indicated by star symbols. The triangles, in panel (d), are for Galactic field RV stars from Lloyd Evans (1985). Error bars are indicated for the LMC CephIIs only if an uncertainty significantly exceeds the size of the symbols. The thick curves are the loci of local giants (see the text for details).

5.1 BL Her and W Vir variables

Fig. 3 shows that in the colour–colour plots the cluster stars are systematically bluer in $H - K_s$ than the local field stars (the thick line). This can be explained, at least in a qualitative sense, by metallicity difference; the locus by Bessell & Brett (1988) is based on local giants probably of solar abundance, while the cluster stars are metal-poor. If we consider giants with different metallicities but with the same surface temperature (in a range of 4000–5500 K), a metal-poor giant is expected to be bluer than a giant with solar abundance in $H - K_s$ but has almost the same colour in J - H (Westera et al. 2002).

In the case of the BL variables, the photometric uncertainties are rather large for the LMC objects, especially in K_s , and it is difficult to discuss the distribution of colours. On the other hand, most of the WV stars in the LMC form a relatively dense grouping in panel (c) of Fig. 3, and many of the globular-cluster stars lie in the same region. There is a conspicuous 'line' of cluster variables to the upper left of the main grouping. We have not found any strong differences between these stars and other cluster WV stars. Two cluster variables are on the extreme left of Fig. 3(c). One of these stars is the variable in the cluster Terzan 1. The reddening of this cluster is high (M06 used $E_{B-V}=2.28$) and probably rather uncertain, and this makes its true position in Fig. 3(c) uncertain. The other star is V129 in NGC 6441. This star lies in a rather crowded region of the cluster, and the colours may be affected by blending.

In Fig. 5, we plot period histograms for CephIIs in the LMC (top panel) and globular clusters (bottom panel). In the LMC histogram,

the pW stars are omitted. The hatched areas indicate the period distribution of the objects whose near-infrared magnitudes are discussed in this study. Several known CephIIs in globular clusters, which were not observed by M06, are collected from the catalogue in P03 and added as the white area in the lower panel. A significant number of short-period BL stars were not included in M06 because of their faintness. The previous surveys of variables with period longer than 1 day are not complete for globular clusters.

Fig. 5 shows a minimum in both the LMC and cluster distributions near 4 days. This is qualitatively consistent with the division between the BL and WV stars as summarized in Section 1. However, there are clear differences between the two distributions at longer periods. In the range $0.6 < \log P < 1.0$, there is an excess of variables in the LMC compared with the clusters. The period distribution of the Galactic field WV stars discussed by Wallerstein & Cox (1984) seems similar to that of the LMC field. However, a caution is required in this comparison since various selection biases will affect the Galactic field sample including the fact that it presumably includes Galactic field pW stars, such as κ Pav. In the LMC, the pW stars are most frequent in the range $0.6 < \log P <$ 1.0. It is notable that a relatively sharp peak at $\log P \sim 1.2$ exists in both panels of Fig. 5. Whilst the deficiency of globular variables in the range $0.6 < \log P < 1.0$ is in broad qualitative agreement with Gingold's models, the excess of variables in this period range in the LMC field (and probably also the Galactic field) is not so easily understood (see Gingold 1985, especially section 9). However, the referee has pointed out to us that the position of the loops found by Gingold is not supported by modern models (e.g. Pietrinferni et al.

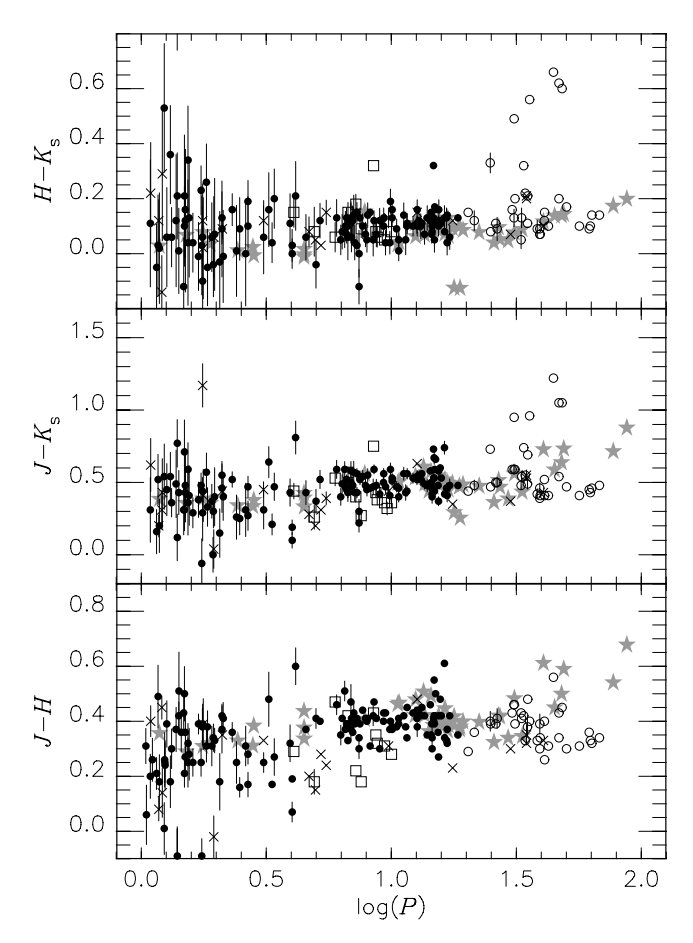


Figure 4. Period–colour relation. Symbols are the same as in Fig. 3. Error bars are indicated for the LMC CephIIs only if an uncertainty significantly exceeds the size of the symbols.

2006). A closer comparison with theory is clearly desirable but outside the scope of this paper. The gap seen in the top panel of Fig. 5 at 20 days, separating the LMC WV and RV stars, is not present in the cluster sample. This will be discussed in Section 5.2.

In Fig. 4, WV stars in the LMC and globular-cluster groups have about the same colours at a given period. In the case of the clusters, however, there is a curious tendency in the range $1.0 < \log P < 1.3$ for (J-H) and $(J-K_s)$ to become bluer with increasing period. This amounts to a change in J-H from ~ 0.45 at $\log P=1.10$ to ~ 0.35 at $\log P=1.25$. Those relatively red objects at around $\log P=1.1$ belong to the outstanding 'line' mentioned above. Whether this feature, which is not shared by the LMC stars, is significant, and if so what it implies remains to be investigated.

5.2 RV Tauri variables

The classical defining feature of RV stars is the alternating depths of the minima in their light curves. However, the distinction between them and the longer period WV stars is not very clear. S08 adopt a division at a period (single cycle) of 20 days. The RV stars are a heterogeneous group as has long been realized (Preston et al. 1963), and at least some are binaries. It is clear from the LMC period—magnitude diagrams (Fig. 2, and fig. 1 of S08) that any PL relation has a considerable scatter though they continue the general increase of brightness with increasing period shown by the shorter period CephIIs. In the case of the JHK_s data, the plots use instantaneous magnitudes for most of the stars, since phase correction is difficult

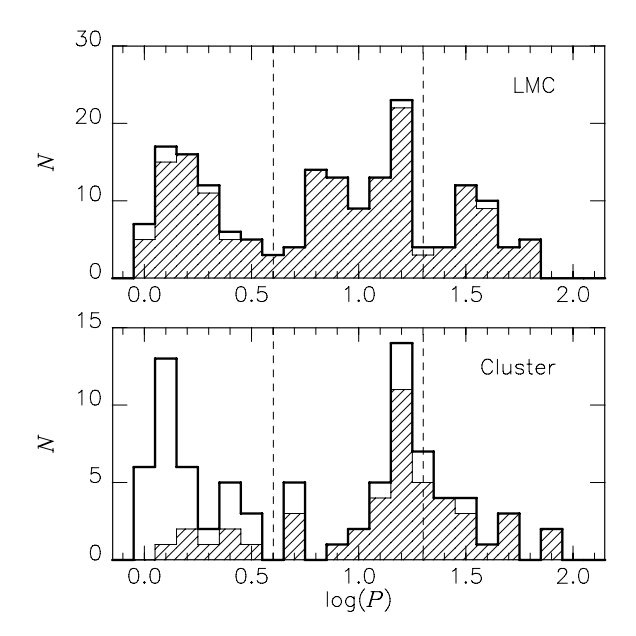


Figure 5. Histograms of periods for the CephIIs: the top panel is for the LMC objects from the S08 catalogue and the lower panel is for those in globular clusters from a combined catalogue of M06 and P03 (see the text for details). The hatched areas indicate the period distribution of the objects whose near-infrared magnitudes are discussed in this study. Vertical lines indicate the period divisions adopted by S08.

for these stars, their periods and light curves tending in many cases to be rather unstable.

It is particularly notable that the RV stars as defined by S08 do not lie on a linear extension of the PL relations defined by shorter period CephIIs (JHK_s and W PL relations). These LMC RV stars all have $\log P$ in the range 1.3 to 1.8. As can be seen from fig. 3 of M06, CephIIs in globular clusters in this period range are colinear with the shorter period stars in JHK_s PL diagrams.

Further evidence for differences between the RV stars in clusters and those in the LMC is found in the period–colour relation (Fig. 4). At the shorter periods among the RV stars, $\log P \le 1.5$, the cluster and LMC stars tend to lie together. They remain together for $\log P > 1.5$ in the case of the $H - K_s$ colours except for the LMC objects with K_s -band excess (see below) but the situation is different in $J - K_s$ and J - H. The cluster RV stars are redder in J - H, while they tend to occupy a region between the bluer LMC stars and those with an infrared excess in the case of $J - K_s$.

The LMC RV stars with the excesses include the three brightest stars at K_s (32, 67, 174). They are also the three reddest stars in Fig. 3, and stand out clearly in the $\log P - K_s$ diagram (Fig. 2). The next two stars which are reddest in $J - K_s$ (both with mild infrared excesses) are numbers 91 and 180. Welch (1987) already noted numbers 67 (HV 915) and 91 (HV 2444) as having infrared excesses. No. 119 (HV 5829) which has a comparable excess to these two stars in Welch's work has the next reddest $H - K_s$ in the IRSF data to the five stars just mentioned.

In the colour–colour diagram (Fig. 3d), the LMC stars with significant K_s excesses lie at $(H - K_s) \sim 0.6$. Most of the others lie relatively close to the intrinsic line, though some may have a very mild excess at K_s . Galactic RV stars from Lloyd Evans (1985), triangles in Fig. 3, show a rather dispersed distribution; their J - H colours range from 0.1 to 0.7 mag. No reddening correction was applied to their colours, and some of the stars may be affected significantly. However, this is not likely to change the overall

impression left by the plot. Whilst there may be some overlap between the three populations (clusters, the LMC and the Galaxy), in general they form distinctly different groupings. Their differences have been also noted by Russell (1998), Zsoldos (1998) and M06.

It should be realized that, in contrast to the LMC and globular-cluster samples, we do not know the absolute magnitudes of the Galactic sample or, indeed, whether they all are in the same evolutionary phase. So far as the cluster RV stars are concerned, we examined the locations of those with periods greater than 40 days, i.e. the most luminous stars of the samples, in K_s –($J-K_s$) diagrams (Matsunaga 2007). They all lie well down the giant branch except possibly for NGC 1904 V8 which is near the top. Thus, these longer period stars in clusters might well be on loops from the AGB like the, shorter-period, WV stars. The histograms of Fig. 5 would be consistent with the view that for P>20 d the cluster variables are simply the long-period tail of the distribution of WV stars, whereas in the LMC there is a distinct population at these periods.

Low-resolution spectra covering the range ∼3800 to 7800 Å of all 36 of the OGLE-III RV stars were obtained in the period 2009 January 16–20, except for numbers 32, 58 and 162. The observations were made with the Cassegrain spectrograph on the 1.9-m reflector at SAAO, Sutherland. No. 15 had strong C2 bands and is the only one of the sample to show C2. Lloyd Evans & Pollard (2004) examined a sample of LMC RV stars, including those discovered in the massive compact halo object survey, and found this star (Macho 47.2496.8) to be the only one in their sample with C2 bands (see also Pollard & Lloyd Evans 2000). However, this star is not particularly outstanding in any of Figs 3 and 4. Note that there must be some overlap between the two samples, although Lloyd Evans & Pollard (2004) do not list the stars they studied. Our spectra show the presence of TiO in numbers 45, 75, 104, 125, 135, 149, 169 and also probably in 25, 51, 112. Since the TiO bands are known to vary in strength with phase, it may well be present in other stars of the sample at other times. Lloyd Evans & Pollard (2004) previously noted weak TiO in 169 = HV 12631. The most sensitive indicator of the presence of TiO in our spectra is the α system sequence beginning near 6159 Å.

6 CONCLUSIONS

We obtained PL relations in phase-corrected JHK_s magnitudes for the combined set of BL and WV stars in the LMC. They have slopes consistent with those found previously (M06) in globular clusters. For the WV stars, the scatter about the PL relations is significantly reduced using the phase-corrected data. The longer period variables (RV stars) show a significant scatter in the infrared and reddeningfree (VI) PL relations, and as a group they are not colinear with the shorter period stars. This contrasts with the situation for CephIIs in globular clusters. It remains to be determined whether those RV stars which do lie near an extrapolation of the PLs from the shorter period can be distinguished from the others in some way, e.g. from radial velocity or spectral features. Differences in infrared periodcolour, colour-colour and period frequency diagrams are found for the WV stars in the LMC and in Galactic globular clusters. In the case of CephII stars with P > 20 d (RV stars), there are marked differences between the available samples in the LMC, Galactic globular clusters and the Galactic field and little evidence that the cluster stars are post-AGB objects. A new class of CephIIs (pW) was identified by S08, and we suggest that the bright Galactic star κ Pav belongs in this class. Such stars have not, so far, been identified in globular clusters and may thus be younger objects.

When the PL relations are calibrated using the pulsation parallaxes of V553 Cen and SW Tau, we find a distance modulus for the LMC of 18.46 \pm 0.10 mag without any metallicity correction, consistent with other recent determinations. Applying our calibration to the CephII stars in the second-parameter globular cluster NGC 6441 leads to a modulus of 15.46 \pm 0.11 mag which confirms the view that the RR Lyraes in this cluster are overluminous for their metallicity.

ACKNOWLEDGMENT

We thank the referee, G. Bono, for his comments and especially for drawing our attention to some theoretical papers.

REFERENCES

Benedict G. F. et al., 2007, AJ, 133, 1810

Bessell M. S., Brett J. M., 1988, PASP, 100, 1134

Bono G., Caputo F., Santolamazza P., 1997, A&A, 317, 171

Bono G., Caputo F., Fiorentino G., Marconi M., Musella I., 2008, ApJ, 684, 102

Caldwell J. A. R., Coulson I. M., 1985, MNRAS, 212, 879

Cardelli J. A., Clayton G. C., Mathis J. S., 1989, ApJ, 345, 245

Carpenter J. M., 2001, AJ, 121, 2851

Di Criscienzo M., Caputo F., Marconi M., Cassisi S., 2007, A&A, 471, 893 ESA, 1997, The Hipparcos Catalogue, ESA SP-1200

Feast M. W., Laney C. D., Kinman T. D., van Leeuwen F., Whitelock P. A., 2008, MNRAS, 386, 2115 (F08)

Freedman W. L. et al., 2001, ApJ, 553, 47

Gingold R. A., 1976, ApJ, 204, 116

Gingold R. A., 1985, Mem. Soc. Astron. Ital., 56, 169

Groenewegen M. A. T., Udalski A., Bono G., 2008, A&A, 481, 441

Kato D. et al., 2007, PASJ, 59, 615

Lloyd Evans T., 1985, MNRAS, 217, 493

Lloyd Evans T., Pollard K. R., 2004, in Kurtz D. W., Pollard K. R., eds, ASP Conf. Ser. Vol. 310, Variable Stars in the Local Group. Astron. Soc. Pac., San Francisco, p. 344

Macri L. M., Stanek K. Z., Bersier D., Greenhill L. J., Reid M. J., 2006, ApJ, 652, 1133

Matsunaga N., 2007, PhD thesis, Univ. Tokyo

Matsunaga N. et al., 2006, MNRAS, 370, 1979 (M06)

Pietrinferni A., Cassisi S., Salaris M., Castelli F., 2006, ApJ, 642, 797

Pollard K. R., Lloyd Evans T., 2000, AJ, 120, 3098

Preston G. W., Krzeminski W., Smak J., Williams J. A., 1963, ApJ, 137, 401 Pritzl B. J., Smith H. A., Stetson P. B., Catelan M., Sweigart A. V., Layden

A. C., Rich R. M., 2003, AJ, 126, 1381 (P03) Russell S. C., 1998, Publ. Astron. Soc. Aust., 15, 189

Schlegel D. J., Finkbeiner D. P., Davis M., 1998, ApJ, 500, 525

Skrutskie M. F. et al., 2006, AJ, 131, 1163

Soszyński I. et al., 2008, Acta Astron., 58, 293 (S08)

Udalski A., Szymański M., Kubiak M., Pietrzyński G., Soszyński I., Woźniak P., Zebrun K., 1999, Acta Astron., 49, 201

van Leeuwen F., Feast M. W., Whitelock P. A., Laney C. D., 2007, MNRAS, 379, 723

Wallerstein G., Cox A. N., 1984, PASP, 96, 677

Welch D. L., 1987, ApJ, 317, 672

Westera P., Lejeune T., Buser R., Cuisinier F., Bruzual G., 2002, A&A, 381, 524

Zsoldos E., 1998, Acta Astron., 48, 775

SUPPORTING INFORMATION

Additional Supporting Information may be found in the online version of this article:

Table 2. The catalogue of S08 sources with IRSF counterparts. Modified Julian Dates (MJD), pulsation phase of the observations,

JHK_s magnitudes and their errors are listed for each IRSF measurement as well as the OGLE-IDs, types and periods. Shifts for the phase corrections obtained from the *I*-band light curves are also listed if available. Nine S08 sources are absent because their IRSF counterparts were not found, and 15 S08 sources are listed twice because they are identified with two counterparts from neighbouring fields of the IRSF survey.

Please note: Wiley-Blackwell are not responsible for the content or functionality of any supporting information supplied by the authors. Any queries (other than missing material) should be directed to the corresponding author for the article.

This paper has been typeset from a $T_EX/I \Delta T_EX$ file prepared by the author.